The continuous swelling-degradation behaviors and chemo-rheological properties of waste crumb rubber modified bitumen considering the effect of rubber size

Ren, S.; Liu, X.; Lin, P.; Wang, H.; Fan, W.; Erkens, S.

Publication date
2021

Document Version
Final published version

Published in
Construction and Building Materials

Citation (APA)
Ren, S., Liu, X., Lin, P., Wang, H., Fan, W., & Erkens, S. (2021). The continuous swelling-degradation behaviors and chemo-rheological properties of waste crumb rubber modified bitumen considering the effect of rubber size. *Construction and Building Materials*, *307*, Article 124966.

Construction and Building Materials 307 (2021) 124966

Contents lists available at ScienceDirect

Construction and Building Materials

journal homepage: www.elsevier.com/locate/conbuildmat

The continuous swelling-degradation behaviors and chemo-rheological properties of waste crumb rubber modified bitumen considering the effect of rubber size

Shisong Ren [a,b], Xueyan Liu [a], Peng Lin [a,*], Haopeng Wang [a], Weiyu Fan [b], Sandra Erkens [a]

[a] Section of Pavement Engineering, Faculty of Civil Engineering & Geosciences, Delft University of Technology, Stevinweg 1, 2628 CN Delft, the Netherlands
[b] Key Laboratory of Heavy Oil Processing, China University of Petroleum, Qingdao, PR China

ARTICLE INFO

Keywords:
Crumb rubber modified bitumen
Swelling
Degradation
Rubber size
Rheology
Chemical characterization

ABSTRACT

The chemo-rheological properties of crumb rubber modified bitumen are always unstable due to the mutable and uncontrollable swelling-degradation degree of crumb rubber in bitumen matrix. The study aimed at exploring the continuous swelling and degradation behaviors of crumb rubber modified bitumen (CRMB) considering the influence of rubber size through monitoring the dynamic viscosity changes of CRMB binders. Moreover, the synergistic effects of swelling-degradation degree and rubber size on the chemical and rheological properties of CRMB were investigated. The results revealed that the rubber size significantly influenced the swelling and degradation behaviors of CRMB. The reduction of rubber size shortened the equilibrium swelling and degradation time, while increased the related viscosity dramatically. Moreover, during the degradation process, the decrease of rubber size could accelerate the continuous swelling rate, increase the maximum viscosity and reduce the continuous swelling time of CRMB. Meanwhile, the high swelling degree and large rubber size were beneficial to enhance the high temperature properties, while the CRMB binder with high degradation degree showed the better low-temperature property, workability and wider Newtonian flow region. Furthermore, the degradation degree promoted the formation of free hydroxide groups, aldehydes, carboxylic acids and esters, while the swelling process increased the average molecular weight of whole liquid phase in CRMB binder. The outputs from this fundamental study are beneficial to provide the guidance to preparation conditions optimization of CRMB binders with different viscous property standards.

1. Introduction

The asphalt pavement exhibits unique characteristics regarding the sufficient predominant driving comfort, bearing capacity and structural stability [1,2], and the bitumen as an essential connector significantly determines the mechanical performance of asphalt mixture [3,4]. However, both terrible environmental and heavy loading conditions invalidate the bonding functions of bitumen in asphalt roads, and several diseases of rutting, cracking and raveling would occur [5,6]. Different types of bitumen modifiers have been utilized, such as the styrene–butadienestyrene (SBS), styrene-butadiene rubber (SBR) and epoxy resin [7–9]. However, the synthesis of these polymer modifiers would consume lots of energy and hydrocarbon products from crude oil [10,11]. Meanwhile, the rapid development of auto industry results in a large number of scrap tires produced, which are always processed with the conventional landfill and incineration methods [12]. Therefore, the develop of crumb rubber modified bitumen is beneficial to bitumen performance improvement and environmental protection.

It has been proved that the incorporation of crumb rubber could strengthen the low-and-high temperature properties of asphalt binder and mixture distinctly [10,13]. Currently, three technical routes regarding the incorporation of crumb rubber into asphalt roads were introduced, including the dry process, wet process as well as Terminal Blend (TB) [14]. Definitely, the rubber powders were added into asphalt mixture directly in the dry process, while the crumb rubber modifier and bitumen were firstly blended before the preparation of asphalt mixture in the wet method. Clearly, the interaction degree between crumb rubber and bitumen in wet method is deeper. Moreover, to improve the worse workability and storage stability of CRMB binder in wet method,

* Corresponding author.
E-mail addresses: Shisong.Ren@tudelft.nl (S. Ren), x.liu@tudelft.nl (X. Liu), P.Lin-2@tudelft.nl (P. Lin), haopeng.wang@tudelft.nl (H. Wang), 15853256892@139.com (W. Fan), S.M.J.G.Erkens@tudelft.nl (S. Erkens).

https://doi.org/10.1016/j.conbuildmat.2021.124966
Received 2 June 2021; Received in revised form 31 August 2021; Accepted 15 September 2021

Nomenclature

CR	Crumb rubber
CRMB	Crumb rubber modified bitumen
SBS	Styrene-butadiene-styrene
SBR	Styrene-butadiene rubber
PET	Polyethylene terephthalate
TOR	Trans-polyoctenamer
DBP	Dibutyl phthalate
S	Saturates
A	Aromatics
R	Resins
At	Asphaltenes
DSR	Dynamic shear rheometer
MSCR	Multiple stress creep and recovery
FTIR	Fourier-transform infrared spectroscopy
GPC	Gel permeation chromatography
THF	Tetrahydrofuran
η	Viscosity
t_s	Swelling time
t_{es}	Equilibrium swelling time
SR	Swelling ratio
η_{max}	Maximum viscosity
η_{equ}	Equilibrium degradation viscosity
DR	Degradation ratio
G*	Complex modulus
G*/sinδ	Rutting factor
R%	Recovery percentage
Jnr	Non-recoverable creep compliance
ZSV	Zero-shear viscosity

the terminal blend (TB) rubber bitumen was developed through increasing the reaction temperature and prolonging the reaction time [15–17]. Hence, the CRMB binders with various reaction conditions would exhibit the different rheological and engineering performance, and the interaction mechanism between the crumb rubber and bitumen plays an important role, which should be further fundamentally understood.

The swelling and degradation procedures are proposed as the interaction mechanisms between the crumb rubber modifiers and bitumen matrix [18,19]. During the blending of CRMB binder, the solid CR particles absorbed the light oily-components from bitumen phase and its occupied volume continued to increase till reaching an equilibrium state. This process is similar to the swelling reaction between the natural rubber and rubber to enhance the plasticity and compatibility during the preparation of rubber products [20–23]. The swelling behavior and its influence on the thermo-rheological properties of CRMB binder have been investigated. It was reported that the swelling of rubber in bitumen had a fast-growing process till reaching the equilibrium status, and the CR modifier was found to absorb only the light components from bitumen phase [24]. Meanwhile, the results from numerical simulation with a finite element model reveled the swelling degree of truck-tire rubber was larger than car-tire rubber. The truck-tire rubber contains more natural rubber than car-tire rubber, which swells faster than the synthetic rubber in bitumen. Besides, it was found that the decrease of rubber particle size led to the faster swelling and earlier equilibrium state of CRMB binder [25].

On the other hand, the increased temperature and extended blending time could both disentangle the crosslinked polymer chains in crumb rubber and the inner molecules were released into the bitumen matrix [26]. The depolymerization and dissolution reactions are known as the degradation procedure, which also plays a dominate role in affecting the chemo-rheological properties of CRMB binders [27–29]. Generally, the gradual degradation of crumb rubber improved the workability and storage stability but sacrificed the rutting resistance [30], but the excessive degradation would deteriorate the high-temperature properties of CRMB binder [31]. The chemical components and physical size of crumb rubber powders both exhibit great influence on the partial dissolution of crumb rubber in bitumen distinctly. Meanwhile, the increasing interaction temperature and mixing rate would promote the desulfurization and depolymerization reactions of polymer chains in rubber, which results in the release of polymeric components of crumb rubber into the bitumen matrix [32,33]. To monitor the chemical and physical change of rubber particles in bitumen during the swelling and degradation processes, the chemical methods of four groups analysis, X-ray photoelectron spectroscopy (XPS), Infrared spectra (IR) and different scanning calorimetry (DSC) were utilized to separated crumb rubber and bitumen phases after the swelling and degradation reactions. In addition, it was found that the swelling process reduced the ductility and penetration indications, while the softening point increased [31,34]. Meanwhile, the viscosity change was validated as a macroscopic reflection of the physical and chemical characterizations of crumb rubber in bitumen [31].

The crumb rubber powder is manufactured by the mechanical crushing, which causes its uneven particle size. Previous studies showed that the rubber size is an important factor to the rheological and mechanical properties of rubber asphalt binder and mixture [35–37]. It was found that the increased rubber particle size could improve the elastic property but deteriorate the fatigue life of rubber binders [35]. At the same time, the CRMB binder with the coarse crumb rubber powders exhibited better rutting resistance, while the reduction of rubber size could enhance the low-temperature fracture property and moisture damage resistivity dramatically [36]. Furthermore, it was also reported that the rubber asphalt mixture with larger rubber size exhibited the better fatigue life and weaker resilient modulus [37]. Hence, the particle size of crumb rubber distinctly influences the chemical compositions, physical and rheological properties of CRMB. Essentially, the rubber size changes the swelling and degradation reaction ways between the bitumen and rubber particles. Nevertheless, there is a lack of research studies regarding the effect of rubber size on the continuous swelling and degradation behaviors of CRMB binders.

The swelling-degradation degree and rubber particle size both distinctly affect the chemo-rheological properties of crumb rubber modified bitumen, and there is a close relationship between rubber size and swelling-degradation degradation behaviors of CRMB binder. However, the continuous swelling and degradation behaviors of CRMB binders with different rubber sizes are still unclear, which results in that there is no basis for optimizing the reaction conditions (temperature and mixing time) of CRMB binders with different viscous performance requirements. Moreover, the properties difference of CRMB binders with various swelling-degradation degrees and rubber size has not been studied yet. It is necessary to fully understand the continuous swelling and degradation behaviors of CRMB binder, which is significantly beneficial to provide the theoretical guidance to the researchers and manufactures for controlling the swelling-degradation degree and preparing the CRMB binders with different rheological characteristics. Therefore, the objectives of this study are to fundamentally explore the continuous swelling and degradation behaviors of CRMB binder considering the influence of rubber size and comprehensively evaluate the synergistic influence of swelling-degradation degree and rubber size on the chemo-rheological properties of CRMB binder.

2. Scope of work

Fig. 1 illustrates the main research methodology of this study. The

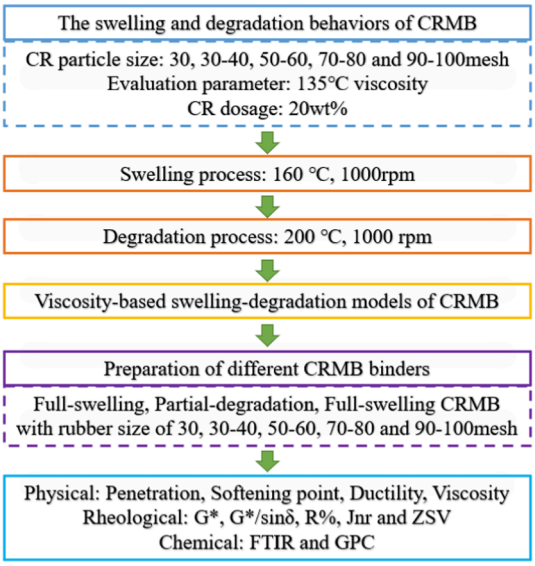

Fig. 1. The research methodology.

viscosity change is monitored to explore the continuous swelling and degradation behaviors of crumb rubber modified bitumen with different rubber sizes of 30, 30–40, 50–60, 70–80 and 90–100 mesh. Based on the previous studies and practical experience, the 160 and 200 ℃ are selected as the temperatures of swelling and degradation procedures. Moreover, the viscosity-based swelling and degradation models of CRMB binders are proposed, which are beneficial to optimize the equilibrium swelling and degradation conditions of CRMB binders with different rubber sizes. Furthermore, the synergistic influence of swelling-degradation degree and rubber size on the chemo-rheological properties of CRMB binders are comprehensively characterized.

3. Materials and methods

3.1. Raw materials

The virgin bitumen with the penetration grade of 60–80 derived from the Marui crude oil was utilized in this study. The physical properties of fresh and aged binders were listed in Table 1, including the 25 ℃ penetration, softening point and 15 ℃ ductility. Meanwhile, the weight percentages of saturates (*S*), aromatics (*A*), resins (*R*) and asphaltenes (*At*) in virgin bitumen were 13.3%, 17.4%, 39.7% and 29.6%, respectively. Moreover, the 30-mesh crumb rubber (CR) powders were manufactured with the ambient grinding process of scrap truck tire. The density of rubber powder was 1.2 g/cm^3 and the weight percentage of moisture, ash, rubber hydrocarbon and carbon element were 0.30, 5.40, 55.8 and 30.2. Table 2 demonstrated the particle size distribution of the crumb rubber, and more than 50 wt% crumb rubber powders showed the particle size higher than 270 μm. The crumb rubber powders with different particle sizes of 30–40, 50–60, 70–80 and 90–100 mesh were separated and collected to further preparation of the CRMB binders with different rubber sizes.

Table 1
The physical properties of virgin and aged bitumen.

Physical properties	Penetration@25 ℃ (0.1 mm)	Softening point (℃)	Ductility@15 ℃ (cm)
Virgin bitumen	67	48.4	135.2
RTFOT-aged bitumen*	41	53.4	36.2
PAV-aged bitumen**	21	63.3	6.2
Test standard	ASTM D5 [38]	ASTM D36 [39]	ASTM D113 [40]

* RTFOT: Rolling Thin Film Oven Test [41]; ** PAV: Pressure Aging Vessel [42].

3.2. Continuous swelling and degradation procedures of CRMB binders

In this study, the continuous swelling and degradation processes of CRMB binders with different rubber particle sizes of 30, 30–40, 50–60, 70–80 and 90–100 mesh were conducted. Firstly, the 20 wt% crumb rubber powders were incorporated into the heated virgin bitumen, and the system temperature rise quickly. Once the temperature reached 160 ℃, the CR/bitumen blend was stirred with a constant speed of 1000 rpm, and then the blending time started to be recorded. During the swelling process of CRMB binder, about 15–20 g specimen was taken out per hour to measure the 135 ℃ rotational viscosity value. When the viscosity value of CRMB binder during swelling procedure showed no change with the increase of swelling time, the equilibrium-swelling specimen with the stable viscosity parameter was obtained and called "full-swelling" CRMB binder.

Afterwards, the reaction temperature was increased from 160 to 200 ℃ to do the degradation procedure. When the temperature reached 200 ℃, the degradation time of CRMB binder started to be noted. During the continuous degradation process, the rotational viscosity value of CRMB during the degradation process was measured per 2.5 h uninterruptedly. When the viscosity value of degraded CRMB binder kept constant, the equilibrium degradation state was approached and the corresponding binder was marked "full-degradation".

3.3. Preparation conditions of different CRMB binders

After the investigation of continuous swelling and degradation behaviors of CRMB binder, the related full-swelling, partial-degradation and full-degradation time could be determined. In detail, the full-swelling CRMB binders with the CR particle sizes of 30, 30–40, 50–60, 70–80 and 90–100 mesh were prepared at 160 ℃ with the swelling time of 8.0, 8.0, 7.0, 6.0 and 3.5 h, respectively. Meanwhile, the degradation durations were determined as 35, 35, 25, 22.5 and 20.0 h for the CRMB specimens. Further, the partial degradation times were determined when the rotational viscosity of degraded CRMB binders were the average values of maximum and equilibrium degradation levels. Finally, the partial-degradation times of CRMB binders were 18, 20, 13, 9.5 and 7.5 h.

3.4. Performance characterization methods

3.4.1. Rotational viscosity

During the continuous swelling and degradation procedures, the 135 ℃ viscosity values of CRMB binders were tracked with a rotational viscometer [43]. The spinning rate of drill was 20 rpm. Besides, the 135 ℃ viscosity of full-swelling, partial-degradation and full-degradation CRMB binders with different CR particle sizes were also measured.

3.4.2. Physical properties

The physical properties, including the 25 ℃ penetration [38], softening point [39] and 5 ℃ ductility [40], of unaged CRMB binders with different swelling-degradation degrees and rubber sizes were examined.

3.4.3. Rheological properties

The dynamic shear rheometer (DSR, TA-HR1) was employed to assess the rheological properties of CRMB binders with the 25 mm parallel diameter and 1 mm gap width [44]. Firstly, the 60 ℃ frequency sweep tests with the frequency region of 0.01–100 rad/s were performed to estimate the complex modulus G* of different unaged-CRMB binders. Besides, the temperature sweep tests with the temperature increasing from 48 to 84 ℃ were conducted to evaluate the rutting resistance of unaged-CRMB binders. Additionally, the 60 ℃ multiple stress creep and

Table 2
The particle size distribution of 30-mesh crumb rubber powders.

Mesh	30–40	40–50	50–60	60–70	70–80	80–90	90–100	>100
Size (μm)	380–550	270–380	250–270	212–250	180–212	160–180	150–160	<150
Percentage	34.35%	22.52%	7.34%	14.24%	2.79%	6.54%	5.27%	6.97%

recovery (MSCR) tests were carried out to measure the recovery percentage R% and non-recoverable creep compliance Jnr of RTFO-aged CRMB binders with two loading stress levels of 0.1 and 3.2 kPa [45]. The 60 ℃ steady-state shear tests were used to investigate the influence of swelling-degradation degree and CR particle size on the flow curve of unaged-CRMB binder. The shear rate increased from 0.001 to 100 s^{-1} [46].

3.4.4. Chemical characteristics

Fourier-transform infrared (FTIR) spectroscopy [47] and Gel permeation chromatography (GPC) [48] were applied to examine the functional group distribution and average molecular weight of CRMB binders. The wavenumbers in FTIR test were in the region of 400–4000 cm^{-1}. Moreover, the selected solvent and flow rate in GPC test were tetrahydrofuran (THF) and 1 ml/min, respectively. In this study, bitumen binders were measured at least three times for each characterization test to ensure the reliability of experimental results.

4. Results and discussion

4.1. Continuous swelling behaviors of CRMB binders with different rubber sizes

It was reported that the crumb rubber size strongly determined the physio-chemical and rheological properties of crumb rubber modified bitumen [34–37]. In this study, the continuous swelling and degradation behaviors of CRMB binders are explored for the first time. Fig. 2 shows the viscosity change of CRMB binders with different CR sizes during the swelling process at 160 ℃. With the swelling time prolongs, the viscosity values of all CRMB binders increase gradually till reaching the maximum point, and then the equilibrium swelling state is attained. The swelling behavior of CRMB binder is significantly related to the enhanced rubber volume and interparticle friction during the swelling procedure. Besides, due to the high-proportion of 30–40 mesh CR particles in the whole mixed rubber powders (30 mesh), the viscosity-swelling time curves of CRMB binders with 30–40 mesh and 30 mesh rubber size are similar. It is worth noting that the swelling behaviors of all CRMB binders can be observed, implying that the swelling reaction is the main reaction mechanism of CRMB binder at low temperatures.

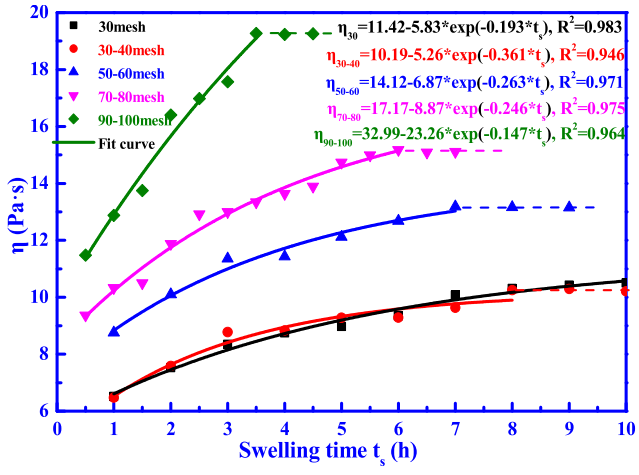

Fig. 2. The viscosity changes of CRMB binder during swelling process.

The continuous swelling behaviors of CRMB binders with various CR sizes are distinctly different. With the CR particle size reduces, the 135 ℃ viscosity of CRMB remarkably increases regardless of the swelling degree. The smaller the CR particle is, the larger the specific surface area is, which strongly enhances the interparticle connection and internal friction resistance. That's why the CRMB binder with smaller CR size shows the higher viscosity. Additionally, it can be found that the swelling rate of CRMB binder with smaller rubber size is faster. The exponential equations are applied to quantitatively assess the swelling behaviors of CRMB binders with different rubber sizes, which are also displayed in Fig. 2. With the CR particle size declines, the absolute b value in the fitting function of "η-t_s" curve decreases. It implies that the viscosity of CRMB with lower rubber size is more sensitive to the swelling time. It is associated with that it is easier for crumb rubber with smaller particle size to reach the swelling equilibrium state because of its limited volume expansion capacity.

To further explore the influence of CR particle size on the "η-t_s" curve of CRMB during the swelling procedure, two parameters of the equilibrium time t_{es} and swelling ratio SR are introduced. Definitely, the equilibrium time is the time point when the viscosity of CRMB binder is independent on the swelling time. Meanwhile, the swelling ratio SR is calculated by dividing the viscosity of full-swelling CRMB binder at swelling time t by which of initial specimen with the general initial swelling time (1 h).

Fig. 3 presents the equilibrium swelling time and swelling ratio parameters of CRMB binders with various rubber sizes. It is illustrated that the crumb rubber size significantly influences the swelling parameters of CRMB binders. The equilibrium swelling time and swelling ratio of 30–40 mesh CRMB binder are both similar to that of 30 mesh sample. The reason is that the mass proportion of 30–40 mesh crumb rubber is the largest in 30-mesh CR powders, which is listed in Table 2. With the reduction of rubber size, the equilibrium swelling time t_{es} remarkably declines. In detail, when the CR mesh is 50–60, 70–80 and 90–100, the corresponding t_{es} is 7.0, 6.0 and 3.5 h, respectively. Hence, it is earlier for CRMB binder with small CR particle size to reach the equilibrium swelling state at a fixed temperature. From Fig. 3, it can be seen that the swelling ratio of CRMB binder reduces as the rubber size decreasing, except for the 90–100 mesh CRMB binder. The crumb rubber powders with smaller particle size would have limited volume to encase the absorbed oily fractions from bitumen matrix. Therefore, it is faster for CRMB with small CR size to attain the equilibrium swelling point, and the final volume of small rubber particle in full-swelling binder is limited, which shortens the equilibrium swelling time and decreases the swelling ratio. Regarding the 90–100 mesh CRMB binder, although the swelling volume of crumb rubber is restricted, the number of CR particles in binder is the largest and the corresponding interparticle distance decreases, which would strengthen the internal friction and viscosity. Herein, the viscosity of full-swelling CRMB binder is associated with the rubber volume, particle number and interparticle force.

Fig. 4 illustrates the 135 ℃ viscosity values of different CRMB binders at the stages of the initial-swelling (when the swelling time is 1 h) and full-swelling (when the viscosity keeps constant). As mentioned before, the viscosity of CRMB binder at the equilibrium point is larger than that of initial sample regardless of the rubber size. Moreover, it can be found that the rubber size strongly affects the initial viscosity η_0 and equilibrium swelling viscosity η_{es}. With the decrease of rubber size, the initial viscosity η_0 and equilibrium swelling viscosity η_{es} of all CRMB binders both increase distinctly, which is related to the higher specific surface area and interparticle friction of rubber particles with lower size.

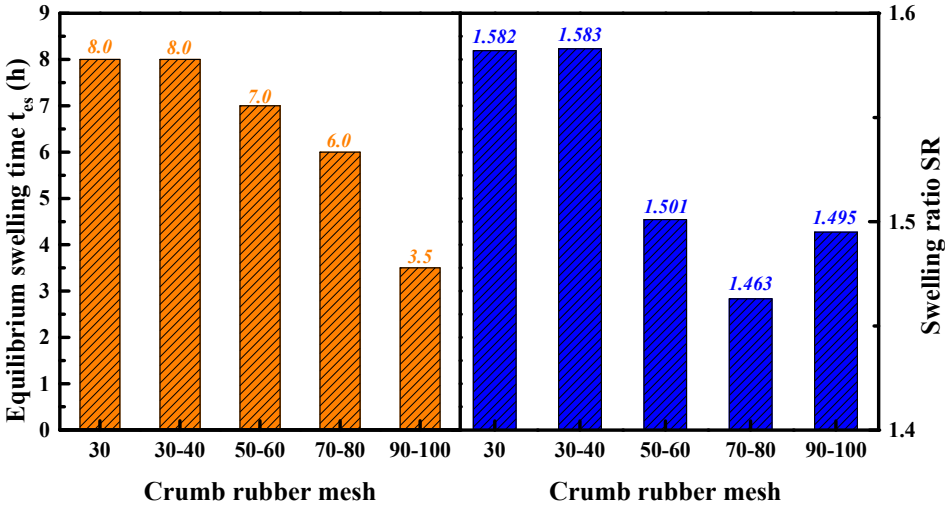

Fig. 3. The equilibrium swelling time and swelling ratio of CRMB binders.

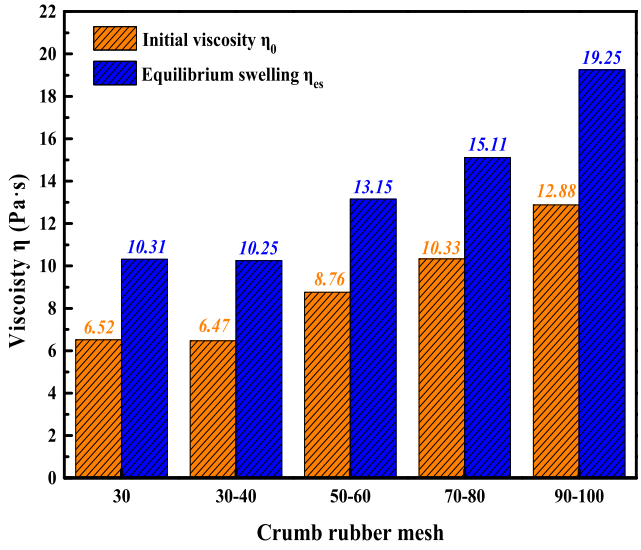

Fig. 4. The initial and equilibrium-swelling viscosity of CRMB binders.

For instance, compared with the 30 and 30–40 mesh CRMB binders, the η_0 and η_{es} values of 90–100 mesh CRMB binder are approximately 2 times higher. Thus, although the reduction of rubber size could shorten the equilibrium time, the increased viscosity of CRMB binder with low rubber size would require the higher temperature for asphalt pavement construction.

4.2. *Continuous degradation behaviors of CRMB binders with different rubber sizes*

The effect of rubber size on the continuous degradation behavior of CRMB binder is also estimated in this study. The viscosity variety of CRMB binders with different CR sizes as a function of the degradation time is shown in Fig. 5a. A viscosity increasing period is observed when the system temperature increases from 160 to 200 ℃, which is associated with the continuous swelling of rubber particles in bitumen due to the thermal expansion and greater molecular motion at high temperatures. Interestingly, for 90–100 mesh CRMB binder, there is no viscosity-increasing stage observed during its degradation procedure. Due to the limitation of free volume in 90–100 mesh rubber particles, the continuous swelling duration is very short, and it is difficult to detect.

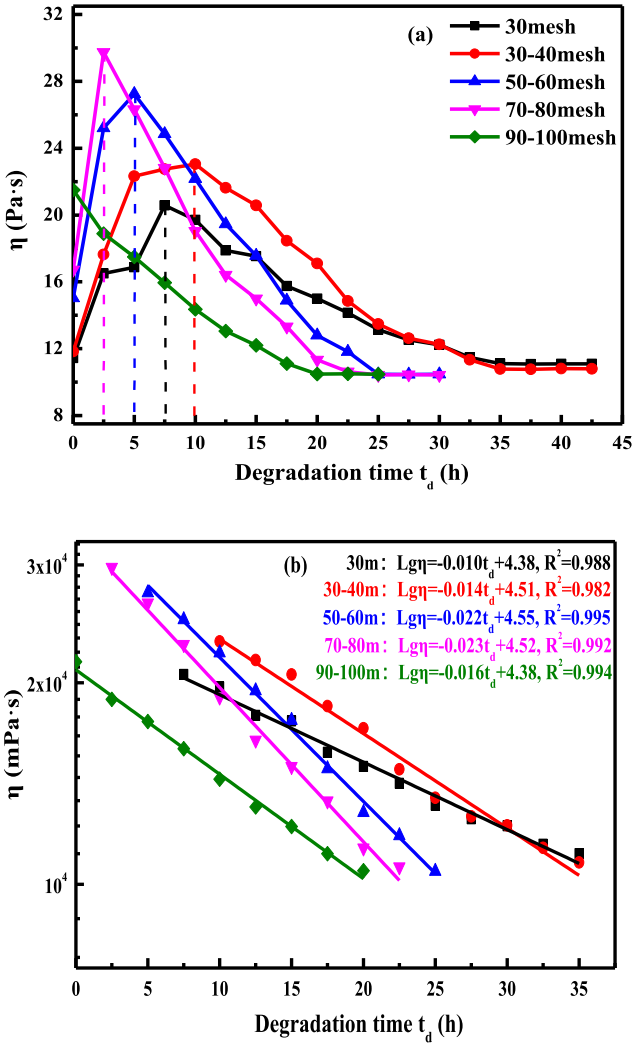

Fig. 5. Influence of degradation time on the viscosity of CRMB binders.

Moreover, the increasing rate of viscosity values for CRMB binders with various CR particle sizes are significantly different, which increases with the reduction of rubber size. The smaller the rubber size is, the larger the

viscosity increasing rate of CRMB binder in the continuous swelling stage.

When reaching the maximum value, the viscosity of CRMB binder starts to decline gradually, and it is the degradation process. It depicts that the viscosity values of different CRMB binders are very similar (about 10.5 Pa·s), regardless of the crumb rubber size. Hence, it can be deduced that the viscosity of full-degradation CRMB binder is not dependent on the rubber size. Due to the long degradation duration, all CRMB binders with different rubber sizes have been completely degraded. Importantly, the rubber size has notable influence on the degradation rate and equilibrium degradation time of CRMB binder. To clearly compare the degradation rate of CRMB binders with different rubber sizes, the "$Lg\eta$-t_d" correlation curves are depicted in Fig. 5b. The logarithmic value of viscosity shows a great linear relationship with the degradation time based on the R^2 value higher than 0.98. Therefore, the semi-logarithm correlation curve between the viscosity and degradation time of CRMB binder is remarkably dependent on the crumb rubber size. It is demonstrated that the absolute slope values in correlation equations of CRMB binders increase with the reduction of rubber size, except for the 90–100 mesh CRMB, which is in the middle between 30 and 40 and 50–60 mesh CRMB binders. Thus, the degradation rate of CRMB binder with smaller rubber size is faster. Meanwhile, the reduction of rubber size would shorten the equilibrium degradation time when the temperature keeps constant. Overall, the rubber size exhibits a significant influence on the degradation rate but not on the viscosity property of full-degradation CRMB binder.

Fig. 6 denotes the degradation parameters of CRMB binders with different rubber sizes, including the maximum swelling time, equilibrium degradation time, maximum viscosity η_{max}, equilibrium degradation viscosity $\eta_{equ}$and degradation ratio DR. The maximum swelling time and equilibrium degradation time are defined as the time when the viscosity value reaches the maximum and equilibrium point, respectively. Herein, the degradation ratio *DR* is calculated as following equation:

$$\text{Degradation ratio} DR = \frac{\eta_{max} - \eta_{equ}}{\eta_{max}} \times 100\% \quad (1)$$

In line with the "viscosity-degradation time" curves, the maximum swelling time of CRMB binders with 30, 30–40, 50–60 and 70–80 mesh rubber size is 7.5, 10.0, 5.0 and 2.5 h, respectively. The continuous viscosity-increasing stage of 90–100 mesh CRMB is too fast to be observed because of the smallest rubber particle size. At the same time, the corresponding maximum viscosity value is 20.58, 23.05, 27.25, 29.75 and 21.50 Pa·s. It should be mentioned that the maximum viscosity of 90–100 mesh CRMB is the instant value when the temperature increases to 200 ℃ because no continuous viscosity-increasing stage is found. Overall, the decrease of rubber size would accelerate the continuous swelling rate and increase the maximum viscosity of CRMB binder during the degradation procedure.

In addition, the equilibrium degradation time of 30, 30–40, 50–60, 70–80 and 90–100 mesh CRMB samples is 35, 35, 25, 22.5 and 20 h, respectively. The low CR particle size is beneficial to promote the swelling and degradation rate of CRMB binder. From Fig. 6c, the degradation ratio of CRMB binders with the crumb rubber size of 30, 30–40, 50–60, 70–80 and 90–100 mesh are 46.1%, 53.2%, 61.6%, 64.3% and 51.3%, respectively. It is worth noting that the degradation ratio of 90–100 mesh CRMB binder is not exact because its maximum viscosity is difficult to be determined. It can be summarized that the CRMB specimen with fine CR particles would show higher degradation ratio at 200 ℃. The smaller the CR size is, the larger the exposed surface area of CR particle is, which enlarges the contact area and solubility of CR modifier in bitumen matrix at high temperatures.

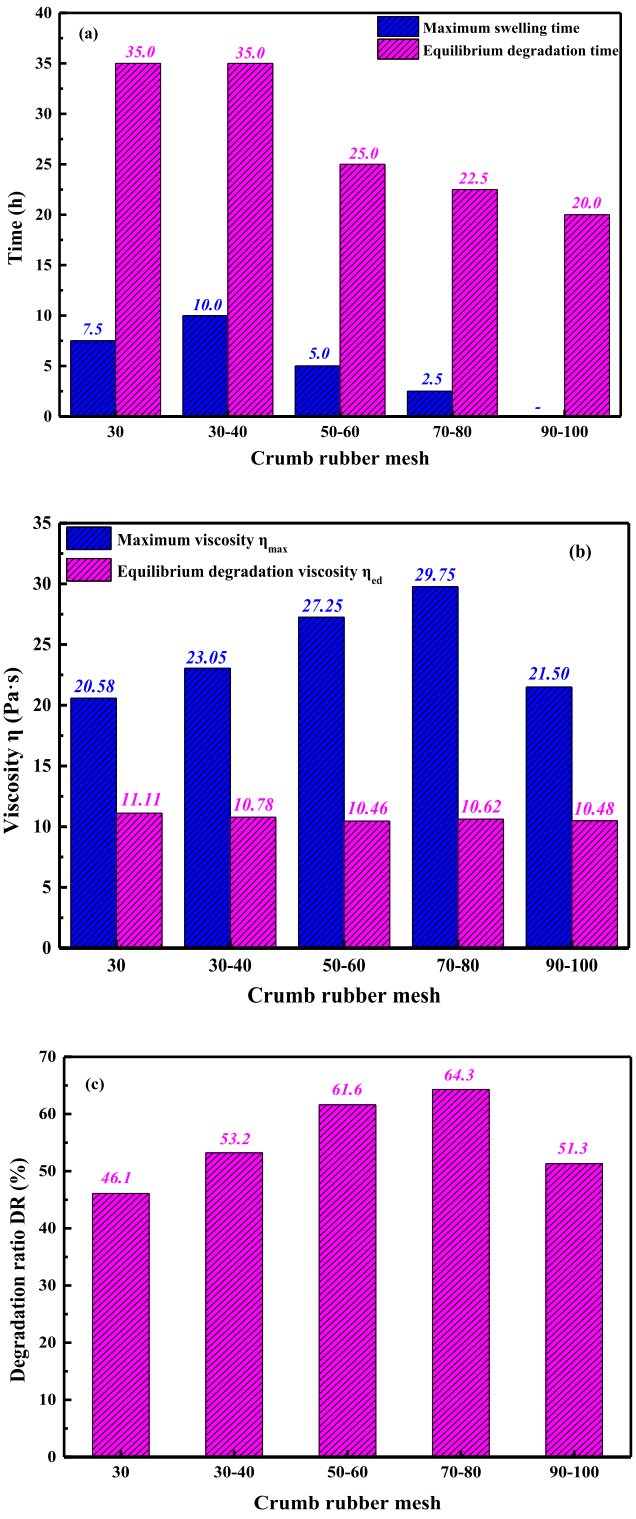

Fig. 6. Influence of rubber size on the maximum swelling time and equilibrium degradation time (a), maximum viscosity and equilibrium degradation viscosity (b), and degradation ratio (c).

4.3. Viscosity-based swelling and degradation models of CRMB binders

The exponential formula and semi-logarithm equation can effectively describe the swelling and degradation behaviors of all CRMB binders with different rubber sizes. Thus, the swelling and degradation models are proposed here to quantitively estimate the influence of swelling-degradation degree and rubber size on the dynamic viscosity of

CRMB binder. The swelling and degradation models are listed as follows:

$$\text{Swellingmodel}: \eta = A + B \times e^{(C \times t_s)} \quad (2)$$

$$\text{Degradationmodel}: Ln\eta = a \times t_d + b \quad (3)$$

where the η is rotational viscosity, Pa·s; t_s and t_d refers to the swelling time and degradation time, respectively, h; and *A, B, C, a* and *b* are all constants.

Table 3 lists the parameters in the swelling and degradation models of CRMB binders with different CR particle sizes. In the continuous swelling models, with the decrease of rubber size, the absolute values of *A* and *B* both increase, but the absolute *C* value decreases gradually. It implies that the CRMB binder with smaller CR particle size would show high viscosity and more sensitive to the swelling time. Moreover, in the continuous degradation model, the reduction of rubber particle size would increase the absolute value of parameters *a* and *b*, when the rubber size is higher than 90–100 mesh. It can be concluded that the decrease of rubber size would shorten both swelling and degradation time, but significantly increase the viscosity of CRMB binder. The proposed exponential swelling and degradation models would be beneficial to optimize the preparation conditions of CRMB binders with specific viscosity standard.

4.4. Effects of swelling-degradation degree and rubber size on physical properties

The physical properties of CRMB binders are characterized to investigate the synergistic effects of swelling-degradation degree and rubber size. According to the results of continuous swelling and degradation behaviors, the preparation conditions for the full-swelling and full-degradation CRMB binders with different rubber sizes could be determined. Moreover, the partial-degradation sample is manufactured when the viscosity is equal to average value between the maximum viscosity η_{max} and equilibrium degradation viscosity η_{ed}. Table 4 summarizes the swelling and degradation time of the full-swelling, partial-degradation and full-degradation CRMB binders with the rubber sizes of 30, 30–40, 50–60, 70–80 and 90–100 mesh. It can be found that the reduction of rubber particle size distinctly shortens the full-swelling, partial-degradation and full-degradation time of CRMB binders.

Fig. 7 shows the physical properties of CRMB binders with different swelling-degradation degrees and rubber sizes, including the 25 ℃ penetratio softening point, 5 ℃ ductility and 135 ℃ viscosity. With the crumb rubber content of 20 wt%, the maximum penetration, softening point, ductility and viscosity values of CRMB binders are 4.6 mm, 84.8 ℃, 16.0 cm and 25.3 Pa·s, respectively. Correspondingly, the minimum values are 2.8 mm, 68.5 ℃, 6.6 cm and 10.2 Pa·s. Thus, the CRMB binder with 20 wt% CR dosage presents the sufficient high-temperature property, but shows the limitations in terms of low-temperature ductility and workability.

It is obvious that the physical properties of CRMB binders significantly depend on the swelling-degradation degree and rubber particle size. The full-swelling CRMB binders exhibit the lower penetration and ductility values than that of partial- and full-degradation samples, regardless of the rubber particle size. It denotes that the degradation stage would decrease the consistency and improve the low-temperature flexibility of CRMB binder. For instance, compared to the full-swelling CRMB binder with the rubber sizes of 30, 30–40, 50–60, 70–80 and 90–100 mesh, the penetration values of corresponding full-degradation sample increase by 0.9, 0.9, 1.2, 1.7 and 1.1 mm, respectively. Similarly, the 5 ℃ ductility of full-degradation CRMB binders are 48.8%, 83.3%, 66.7%, 62.7% and 77.8% higher than that of full-swelling binders.

Table 4
The preparation conditions for different types of CRMB binders.

CR size (mesh)	30	30–40	50–60	70–80	90–100
Full-swelling time (h)	8.0	8.0	7.0	6.0	3.5
Partial-degradation time (h)	18.0	20.0	13.0	9.5	7.5
Full-degradation time (h)	35.0	35.0	25.0	22.5	20.0

With the reduction of rubber particle size, the penetration and ductility values of CRMB binder both increase apart from the penetration of full-swelling binder. When the rubber mesh increases from 30 to 40 to 90–100, the penetration value increases by 0.3, 0.6 and 0.4 mm, while the 5 ℃ ductility increases by 2.4, 2.0 and 3.9 cm for the full-swelling, partial-degradation and full-degradation CRMB binder, respectively. Therefore, the CRMB binder with small rubber size and high degradation degree would present the better low-temperature cracking resistance.

In addition, the swelling-degradation degree and rubber size both exhibit distinct influence on the softening point and viscosity of CRMB binder. Compared to the full-swelling and partial-degradation samples, the softening point and viscosity of full-degradation CRMB are lower, which demonstrates that the degradation procedure would deteriorate the high temperature property but improve the workability of CRMB binder. Interestingly, for 30, 30–40 and 50–60 mesh CRMB samples, the softening point and viscosity of partial-degradation sample are even higher than the full-swelling specimen. The reason may be related to that the high degradation temperature further accelerates the swelling of rubber particles in bitumen matrix. Moreover, the influence law of rubber size on the softening point and viscosity is not apparent. In summary, the high swelling degree of CRMB binder is beneficial to its high-temperature deformation resistance. However, when considering the low-temperature flexibility and workability, the CRMB binder with high degradation degree and small rubber size is recommended.

4.5. Effects of swelling-degradation degree and rubber size on rheological properties

4.5.1. Complex modulus

The frequency sweep test was conducted to assess the complex modulus of CRMB binders with different swelling-degradation degrees and rubber sizes. The results are illustrated in Fig. 8. As expected, the complex modulus of CRMB binder shows a linear increasing trend as the loading frequency increasing with the correlation coefficient R^2 value larger than 0.997. Besides, the frequency-dependence is examined through comparing the slope values in correlation equations. The slope values of all full-degradation CRMB binders are higher than that of full-swelling samples, which manifests that the frequency dependence of complex modulus tends to increase with the deepening of degradation degree. It is noteworthy that the frequency-dependence of complex modulus for the 30, 30–40 and 50–60 mesh partial-degradation CRMB

Table 3
The swelling and degradation models of CRMB binders.

Parameters	Mesh	30	30–40	50–60	70–80	90–100
Swelling model	*A*	11.42	10.49	14.12	17.17	32.99
$\eta = A + B*\exp(C*t_s)$	*B*	−5.83	−5.26	−6.87	−8.87	−23.26
	C	−0.193	−0.361	−0.263	−0.246	−0.147
Degradation model	*a*	−0.0101	−0.0141	−0.0215	−0.0231	−0.0156
$Ln\eta = a*t_d + b$	*b*	4.384	4.507	4.525	4.554	4.384

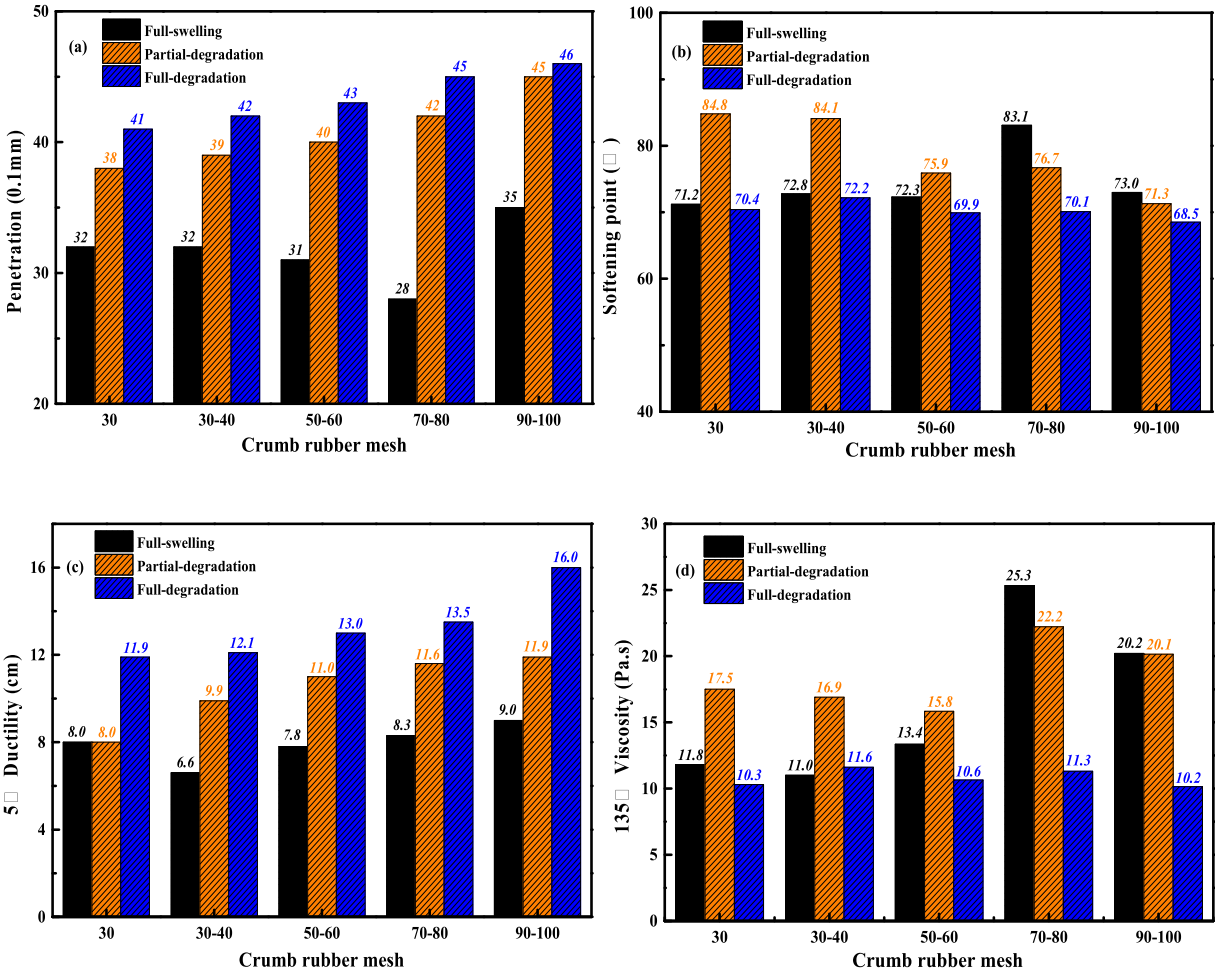

Fig. 7. The physical properties of CRMB binders.

binders are larger than that of corresponding full-swelling samples, which is consistent to the physical properties mentioned before. Thence, the swelling degrees of the 30, 30–40 and 50–60 mesh partial-degradation CRMB binders are higher than the full-swelling samples. Moreover, the rubber size shows no obvious influence on the complex modulus frequency dependence of full-swelling and partial-degradation CRMB binders. Regarding the full-degradation samples, with the reduction of rubber size, the frequency-dependence characteristic of complex modulus becomes more obvious.

Additionally, the complex modulus of full-degradation CRMB binder is much lower than that of full-swelling and partial-degradation samples in spite of the rubber size and loading frequency. It reveals that the degradation procedure adversely influences the complex modulus and deformation resistance of CRMB binder. Meanwhile, the complex modulus values of full-swelling and partial-degradation samples with 30, 30–40 and 50–60 mesh rubber size are similar. However, their reaction mechanisms are completely different. For the full-swelling sample, the swelling degree is the largest at 160 ℃, but the partial-degradation CRMB binder is subjected to the continuous swelling followed by the partial degradation duration at 200 ℃. For the 70–80 and 90–100 mesh CRMB binders, the complex modulus of full-swelling binder is much higher than that of partial- and full-degradation samples, which depicts that the full-swelling CRMB binder shows larger stiffness and permanent deformation resistance. At the same time, the gap between the G^* values of partial- and full-degradation CRMB binders becomes smaller.

With the reduction of rubber size, the G^* values of full-swelling and partial-degradation CRMB binders increase first and then decrease, while that of full-degradation CRMB samples decrease consistently. The G^* values of full-swelling, partial-degradation and full-degradation CRMB binders reach the maximum point when the rubber size is 70–80, 50–60 and 30–40 mesh, respectively. It is notable that the 135 ℃ viscosity and 60 ℃ complex modulus of all full-degradation CRMB binders are similar, which approaches to 10.5 Pa·s and 2 kPa at 0.1 rad/s. Therefore, the influence of rubber size is not considerable when the CRMB binder approaches to the equilibrium degradation state.

4.5.2. *Rutting factor and failure temperature*

To estimate the couple influence of swelling-degradation degree and rubber size on the temperature-sensitivity and rutting resistance of CRMB binder, the temperature sweep tests were performed and the correlations between the rutting factor $G^*/\sin\delta$ and temperature are illustrated in Fig. 9. It is demonstrated that the $G^*/\sin\delta$ values of CRMB samples decrease linearly as the temperature rising, which is associated with the reduction of molecular interaction under high temperatures. That's why the rutting disease of asphalt pavement would occur easily at high temperature. The linear correlation formulas regarding the $G^*/\sin\delta$ of CRMB binders with temperature are also displayed in Fig. 9. The temperature sensitivity of 30 mesh CRMB binders with different swelling-degradation degrees are similar. For the 30–40, 50–60 and 70–80 mesh CRMB binders, the $G^*/\sin\delta$ parameter is more dependent on the temperature with the degradation degree deepening. However, the temperature susceptibility of $G^*/\sin\delta$ for full-degradation 90–100 mesh sample is less obvious than the full-swelling and partial-degradation binders. Further, the rubber size has no visible influence on the temperature sensitivity of CRMB binder.

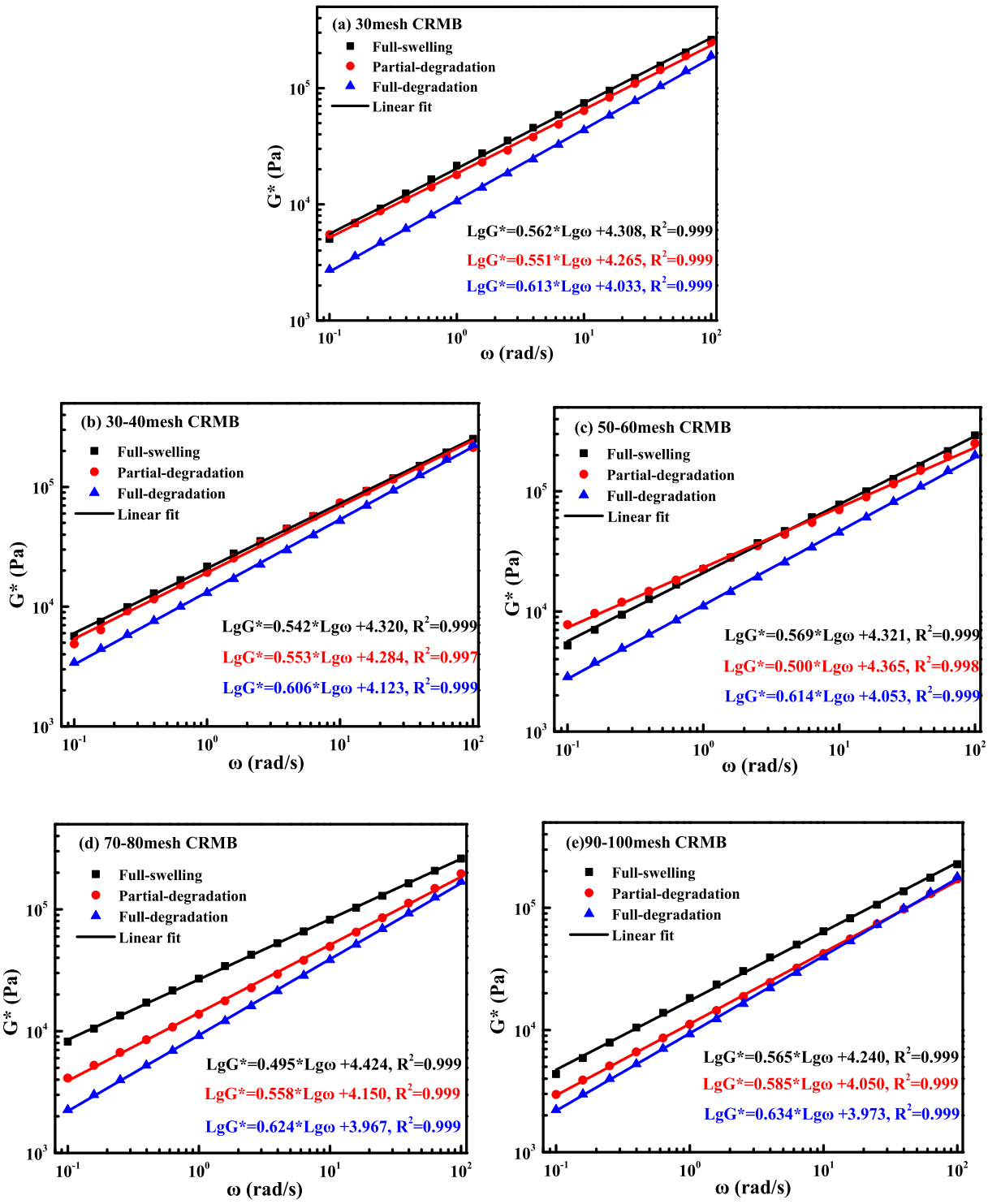

Fig. 8. The complex modulus of CRMB binders.

The $G^*/sin\delta$ values of the full-swelling, partial- and full-degradation CRMB binders are remarkably different. When the temperature is the same, the order of $G^*/sin\delta$ is as following: full-swelling > partial-degradation > full-degradation CRMB binder. The full-swelling CRMB binder exhibits the best rutting resistance, which weakens during the degradation procedure. With the increase of degradation degree, the polymer network in crumb rubber is disrupted gradually, accompanied by the reduced dimension and released light-weight components. The collapse of rubber structure deteriorates its filling-function and interparticle-force. Meanwhile, the released components would soft the bitumen matrix. Both of them contribute to the exacerbation of rutting resistance for full-degradation CRMB binder. When the rubber size decreases from 30 to 40 to 50–60, 70–80 and 90–100 mesh, the $G^*/sin\delta$ values of full-swelling CRMB binders increase by 9.7%, 30.35% and decrease by 16.89%, respectively. Besides, the $G^*/sin\delta$ values of partial-degradation samples decrease by 0.27%, 40.56% and 49.97%, while the $G^*/sin\delta$ values of full-degradation binders decrease by 17.87%, 28.17% and 52.43%. It can be summarized that the decrease of rubber size would obviously weaken the rutting resistance of partial- and full-degradation CRMB binders.

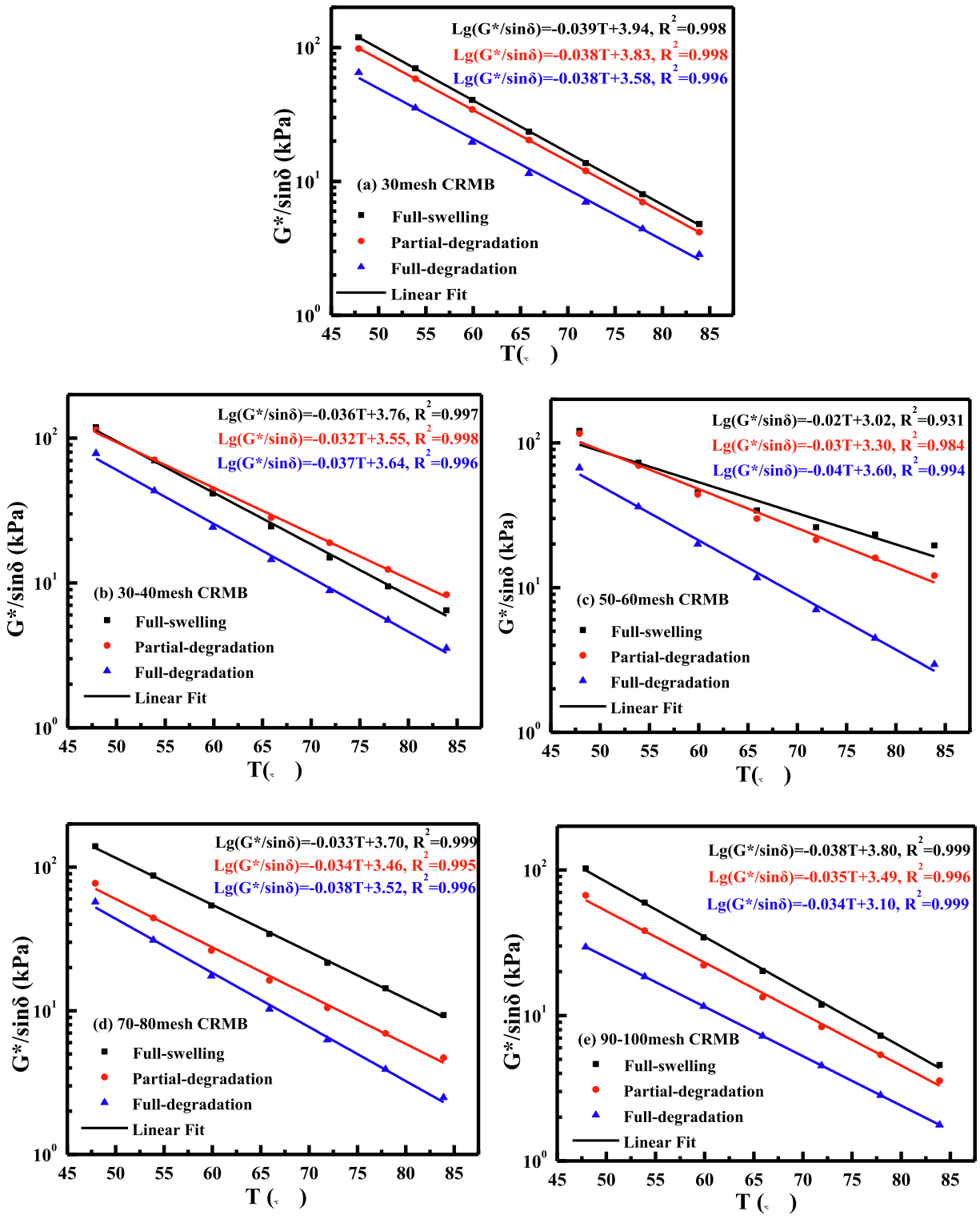

Fig. 9. The relationship between temperature and rutting factors of CRMB binders.

The rutting failure temperatures of CRMB binders are plotted in Fig. 10, which is defined as a certain temperature when the rutting factor *G*/sinδ* value is equal to 1.0 kPa. It can be seen that all CRMB binders have the superior failure temperature higher than 91.1 ℃, which implies that the CRMB binders with 20 wt% CR dosage exhibit the adequate rutting resistance, regardless of the swelling-degradation degree and rubber size. The rutting failure temperatures of CRMB binders with various swelling-degradation status and rubber particle sizes show a great difference. When the rubber size is the same, the full-swelling CRMB binder presents the maximum failure temperature, followed by the partial-degradation binder, while the full-degradation sample shows the minimum value. For the CRMB binders with 30–40 and 70–80 mesh, the failure temperature of partial-degradation sample is 6.9 ℃ and 10.3 ℃ lower than that of full-swelling one, while the failure temperature of full-degradation sample decreases by 15.1 ℃ and 19.7 ℃, respectively. Meanwhile, as the rubber size decreasing, the rutting failure

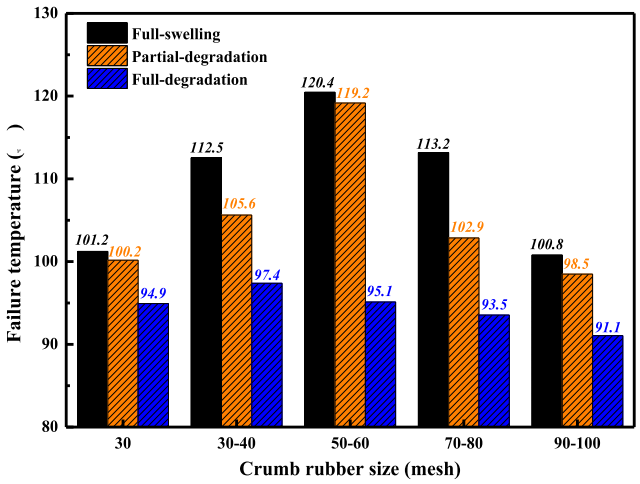

Fig. 10. The rutting failure temperatures of CRMB binders.

temperatures of full-swelling and partial-degradation CRMB binders increase first and then decrease, and the CRMB binders with the rubber size of 50–60 mesh show the maximum value. Moreover, the full-degradation CRMB binder with smaller rubber particle size has the lower rutting failure temperature. However, the influence of rubber size on the rutting resistance of full-degradation CRMB binders is slight, and their rutting failure temperatures are similar, which is consistent to the aforementioned viscosity results.

4.5.3. Elastic recovery and creep compliance

In this study, the multiple stress creep and recovery (MSCR) tests were carried out for measuring the vital parameters of CRMB binders, including the elastic recovery *R%* and non-recoverable creep compliance *Jnr*. Generally, the bitumen binder with the higher *R%* and lower *Jnr* value would exhibit better elastic deformation resistance. The *R%* and *Jnr* parameters of different CRMB binders at two stress levels of 0.1 and 3.2 kPa are displayed in Fig. 11. As expected, the increase of loading stress would decrease the *R%* and *Jnr* values of all CRMB binders, which is related to the larger degree of deformation under the high loading stress. For instance, when the loading stress increases from 0.1 to 3.2 kPa, the *R%* value of 30 mesh full-swelling, partial-degradation and full-degradation CRMB binder decreases by 6.2, 7.6 and 13.5%, respectively. Meanwhile, the corresponding *Jnr* value increases by 64.7, 67.2 and 45.1 times.

It can be found that the swelling-degradation degree and rubber size both influence the creep and recovery behaviors of CRMB binders dramatically. The recovery percentage values of CRMB binders with 20 wt% CR dosage differ from 75.0% to 89.1% at 0.1 kPa and from 63.8% to 67.2% at 3.2 kPa. And the creep compliance values are in the region of 0.39–2.46 Pa and 13.6–105.8 Pa. Besides, when the rubber size is the same, the *R%* value of full-swelling CRMB is the largest, which decreases gradually during the degradation procedure. Correspondingly, the *Jnr* value of full-swelling CRMB is smaller than that of partial- and full-degradation samples. Compared to the full-swelling sample with rubber size of 50–60 mesh, the $R_{0.1}$ and $R_{3.2}$ values of full-degradation CRMB binder decline by 8.9% and 12.9%, while the corresponding $Jnr_{0.1}$ and $Jnr_{3.2}$ values increase by 3.30 and 4.46 times, respectively. However, it is worth mentioning that the influence of swelling-degradation degree on R% and Jnr is not obvious than that of loading stress.

It is demonstrated that both *R%* and *Jnr* of CRMB binders with different rubber sizes have a significant difference, which depends on the loading stress level. The full-swelling CRMB binders with the rubber size of 30–40, 50–60 and 70–80 mesh show the similar *R%* value, while the *R%* of 90–100 mesh full-swelling sample is the lowest. Meanwhile, the influence of rubber size on the *R%* of full-degradation CRMB binder

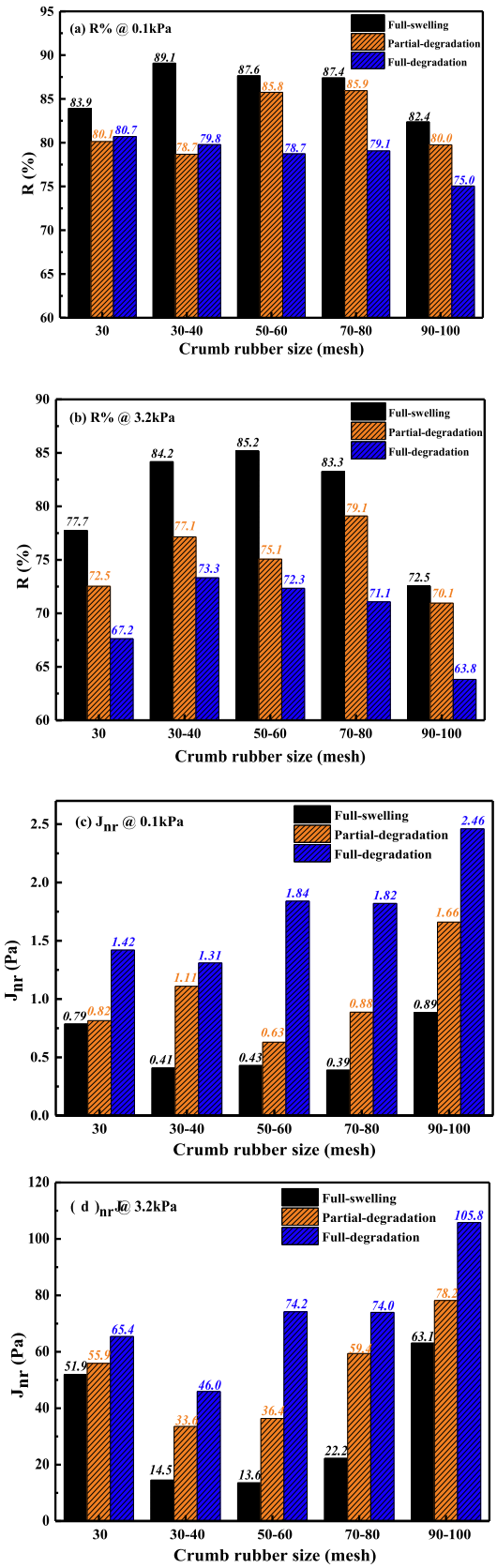

Fig. 11. The recovery percentage R% and creep compliance Jnr of CRMB binders.

is limited. Interestingly, the *R%* values of partial-degradation CRMB binders with the rubber size of 50–60 and 70–80 mesh are higher than that of 30–40 and 90–100 mesh specimens, which is consistent to the aforementioned results of viscosity and rutting factor. Despite the swelling-degradation degree, the CRMB binders with 90–100 have the smallest *R%* values. Herein, the reduction of rubber size would deteriorate the elastic property of CRMB binders.

From Fig. 11, the influence of swelling-degradation degree and rubber size on the creep compliance of CRMB binders is observed. On the whole, the full-swelling CRMB binder has the lowest *Jnr* value, while

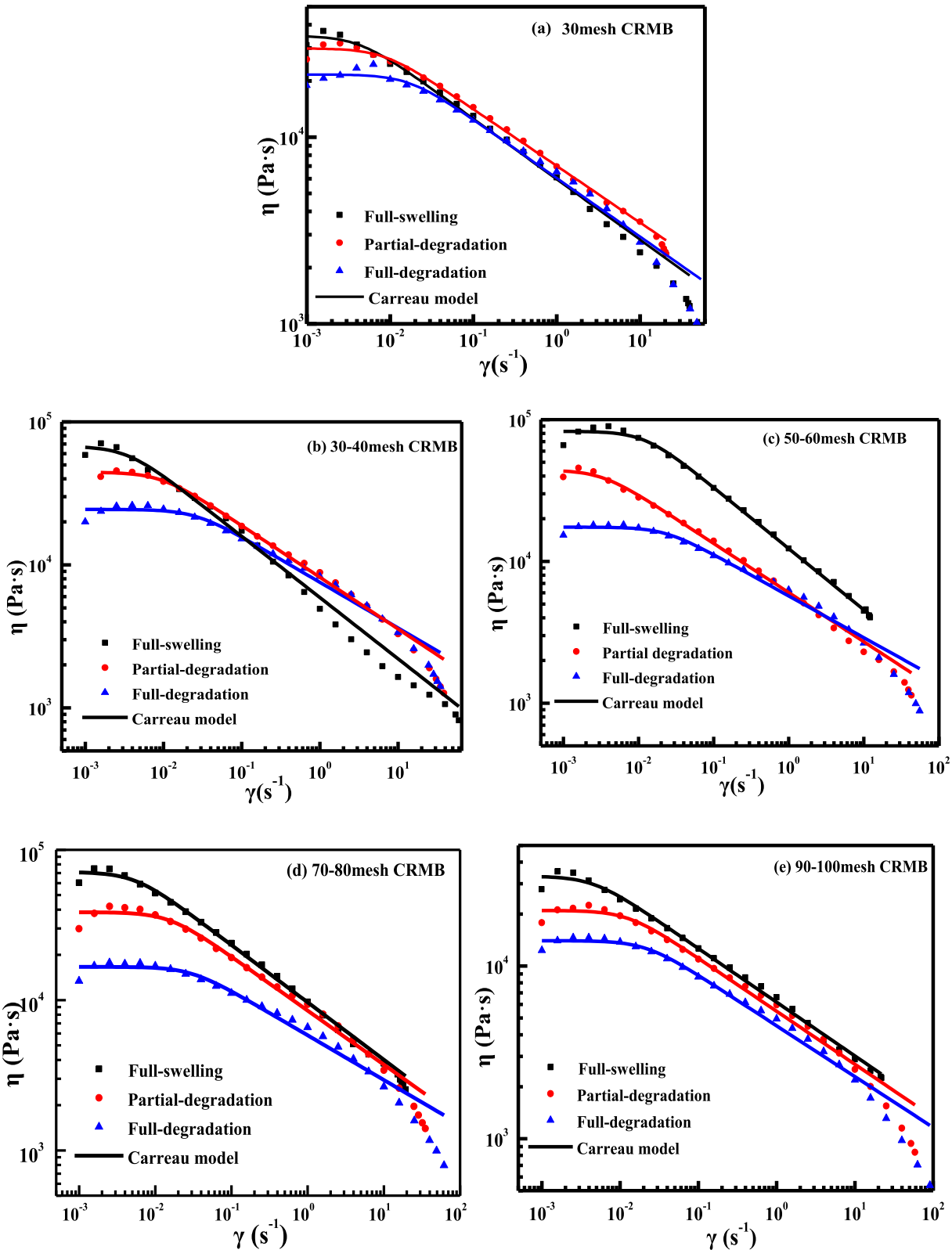

Fig. 12. Flow curves of CRMB binders.

the full-degradation sample presents the highest *Jnr* value. It implies that the degradation process would increase the viscous proportion in CRMB binder and increase the risk of permanent deformation. The influence of rubber size is more obvious when the stress level is 3.2 kPa. The decrease of rubber size leads to the improvement of *Jnr* value. When the rubber size is smaller, it is easier for rubber particles to degrade in bitumen matrix, which results in more viscous component released. The full-degradation CRMB binder with the rubber size of 90–100 mesh shows the maximum *R%* and minimum *Jnr* value. Moreover, the full-swelling CRMB binder with the rubber size of 30–40 or 50–60 mesh have the highest *R%* and lowest *Jnr* value. From the viewpoint of deformation resistance, the CRMB binder with large rubber size and high swelling-degradation ratio is the best.

4.5.4. Flow curve and zero-shear viscosity

Generally, the bitumen binder is a representative non-Newtonian and pseudoplastic fluid, and its viscosity obviously depends on the shear rate. In this study, the steady-state flow tests were performed to assess the flow behaviors of CRMB binders with various swelling-degradation degrees and rubber sizes, which are shown in Fig. 12. As expected, the complex viscosity values of CRMB binders decrease significantly as the shear rate increasing. However, when the shear rate is lower than 0.01 s^{-1}, there is a stable platform where the viscosity of CRMB binder has no change with shear rate. It indicates that the CRMB binder exhibits the characteristics of Newtonian fluid. The swelling-degradation state remarkably influences the complex viscosity values and flow curves of CRMB binders. In most cases, the full-degradation CRMB binder exhibits the lower complex viscosity than that of full-swelling and partial-degradation specimens, which agrees well with the rotational viscosity results. Hence, the prolonged degradation degree is beneficial to reduce the complex viscosity and enhance the workability of CRMB binder. In addition, with the increase of shear rate, the effect of swelling-degradation degree on the viscosity of CRMB binder becomes inconspicuous. Interestingly, the increased degradation degree enlarges the Newtonian flow region. The rubber size in full-degradation CRMB binder is smaller than that in full-swelling and partial-degradation samples, which contributes to the improved viscous flow characteristic of CRMB binder.

The Carreau model is utilized to fit the correlation curve regarding the complex viscosity with shear rate for CRMB binder, which is as follows:

$$\frac{\eta_0}{\eta} = \left[1 + \left(\frac{\gamma}{\gamma_c}\right)^2\right]^s \tag{4}$$

where η is the complex viscosity of CRMB binder, Pa·s; γ refers to the shear rate, s^{-1}; η_0 represents the zero-shear viscosity (ZSV), Pa·s; γ_c and s are constants. Besides, the zero-shear viscosity is defined as the complex viscosity when the external shear rate approaches to zero. Moreover, the parameter s refers to the falling slope of the viscosity and the γ_c is the shear rate value when the shear-thinning behavior of CRMB binder appears. The non-Newtonian behavior of bitumen sample with higher s and lower γ_c value is more distinct.

Table 5 lists the Carreau model parameters of flow curves for CRMB binders with different swelling-degradation degrees and rubber sizes. The Carreau model can fit the flow curve of CRMB binder well with the R^2 values larger than 0.97. The swelling-degradation degree affects the Carreau model parameters s and γ_c of CRMB binders dramatically. When the rubber size is the same, the full-swelling CRMB binder has the lowest γ_c and highest s value, while the full-degradation sample shows the maximum γ_c and minimum s values. Moreover, the values of s and γ_c parameters for partial-swelling ones are in the middle. For instance, compared to the 30–40 mesh full-swelling CRMB binder, the s value of corresponding partial- and full-degradation sample decreases from 0.214 to 0.181 and 0.160, while the γ_c parameter increases from 0.004 to 0.009 and 0.025 s^{-1}, respectively. It implies that the full-swelling CRMB binder exhibits the wider non-Newtonian region than the partial and full-degradation specimens, while the shear rate susceptibility of the latter is less obvious than the former. Therefore, the degradation process would enhance the Newtonian flow region because of the decreased polymer network density and increased light-components in the bitumen matrix.

Additionally, the flow parameters of CRMB binders are strongly associated with the rubber size. With the decrease of rubber size, the s value decreases gradually. The 30–40 mesh CRMB binder exhibits the highest s value, regardless of the swelling-degradation degree. Meanwhile, the s value of 90–100 mesh CRMB is the lowest. Hence, the flow curve of CRMB binder with the larger rubber size would be more susceptible to shear rate and shows more distinct shear-thinning behavior. Besides, the γ_c parameter of CRMB binder rises with the reduction of rubber size. Moreover, the 70–80 and 90–100 mesh CRMB binders have the similar γ_c value. The Newtonian flow range of CRMB binder with the smaller rubber size is wider. Furthermore, the influence of rubber size on the flow parameters of full-degradation CRMB binder is less obvious than that of full-swelling and partial-degradation samples. The rubber particles in full-degradation samples are maximally dissolved in bitumen matrix, and the effects of rubber size on the rheological properties of CRMB binder are weakened. Meanwhile, the influence of rubber size on the s value of CRMB binder is more distinct than the γ_c parameter.

Fig. 13 depicts the zero-shear viscosity (*ZSV*) of CRMB binders with various swelling-degradation degrees and rubber sizes. It can be found that the *ZSV* values of CRMB binders are all higher than 14000 Pa·s, indicating that the CRMB with CR dosage of 20 wt% exhibits the sufficient shear deformation resistance. The swelling-degradation degree significantly affects the *ZSV* value of CRMB. For all CRMB binders with different rubber sizes, the full-swelling sample shows the highest *ZSV* value, which declines with the degradation degree deepening

Table 5
The flow curve parameters of different CRMB binders.

Mesh	Parameters	30	30–40	50–60	70–80	90–100
Full-swelling CRMB binders	γ_c (s^{-1})	0.004	0.004	0.003	0.005	0.005
	s	0.162	0.216	0.214	0.191	0.156
	R^2	0.990	0.987	0.990	0.987	0.984
Partial-degradation CRMB binders	γ_c (s^{-1})	0.008	0.009	0.012	0.015	0.013
	s	0.157	0.181	0.173	0.180	0.153
	R^2	0.990	0.996	0.981	0.976	0.987
Full-degradation CRMB binders	γ_c (s^{-1})	0.017	0.025	0.022	0.029	0.028
	s	0.152	0.160	0.147	0.149	0.147
	R^2	0.980	0.980	0.988	0.977	0.990

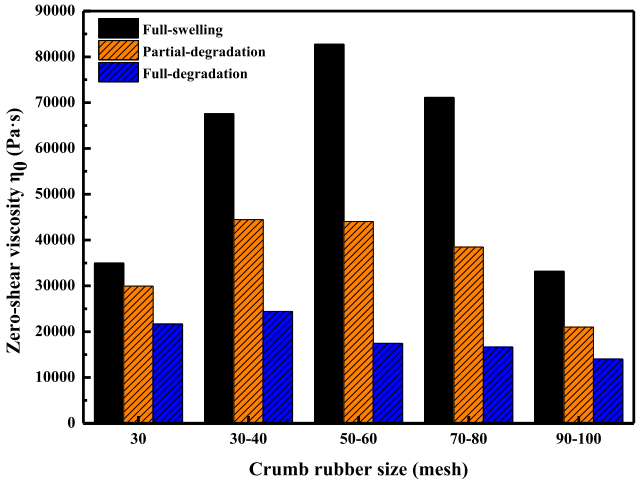

Fig. 13. The zero-shear viscosity η_0 values of CRMB binders.

dramatically. Compared to the full-swelling CRMB with the rubber size of 30, 30–40, 50–60, 70–80 and 90–100 mesh, the *ZSV* value of corresponding partial-degradation sample decreases by 14.4%, 34.2%, 46.8%, 46.0% and 36.7%, respectively. Meanwhile, the related *ZSV* value of full-degradation CRMB is 38.0%, 63.9%, 78.9%, 76.6% and 57.7% lower than full-swelling specimen. Moreover, the rubber size has an obvious influence on the *ZSV* parameter of CRMB binder, especially for the full-swelling and partial-degradation samples. Regarding the full-swelling CRMB binders, with the decrease of rubber size, the *ZSV* value increases first and then decreases, which reaches the maximum point when the rubber size is 50–60 mesh. When the rubber size decreases from 30 to 40 to 50–60, 70–80 and 90–100 mesh, the *ZSV* value of partial-degradation sample reduces by 0.9%, 13.4% and 52.76%, and the *ZSV* value of full-degradation CRMB binder decreases by 28.6%, 31.8% and 45.5%, respectively. Therefore, the increasing degradation degree and decreasing rubber size would weaken the deformation resistance but improve the workability of CRMB binder.

4.6. Effects of swelling-degradation degree on chemical properties

To explore the influence of swelling-degradation degree on the chemical functional groups and average molecular weight of CRMB binder, the Fourier-transform infrared (FTIR) spectroscopy and Gel Permeation Chromatography (GPC) methods were performed. Four CRMB binders with the rubber size of 30 mesh and different swelling-degradation degrees were selected. The swelling time of partial-swelling and full-swelling samples are 0.5 and 8.0 h, while the degradation duration of partial-degradation and full-degradation are 7.5 and 35 h, respectively.

4.6.1. Functional groups distribution

Fig. 14 illustrates the FTIR curves of CRMB binders with different swelling-degradation degrees. The broad peak at 3300–3400 cm^{-1} reflects the stretching vibration absorption of CHOH functional groups. The high degradation degree results in the shift left of this peak, indicating that the free hydroxide groups are created during the degradation process of CRMB binder. As expected, the two main peaks at 2920 and 2852 cm^{-1} come from the C–H stretch of alkanes in bitumen. The specific peak at 1730 cm^{-1} refers to the stretch of C = O functional group in aldehydes and carboxylic acids. Interestingly, the full-degradation CRMB binder has the largest absorbance of C = O group, and oxidation reaction would occur during the degradation procedure of CRMB binder.

The swelling-degradation degree has no significant effect on the C = C stretch in alkenes and alkynes according to the functional group peaks at 1640, 1600 and 1452 cm^{-1}. It is worth mentioning that the peak absorbance of 1160 cm^{-1} in full-degradation CRMB is the largest, which represents the C-O-C stretch in esters. Moreover, the formation of ester functional groups in CRMB binder strengthens as the degradation degree deepening. Compared to swelling sample, the absorbance of functional groups S = O in degradation one is lower. It validates that the desulfurization reaction would occur during the degradation duration of CRMB. In summary, the degradation process would accelerate the formation of aldehydes, carboxylic acids and esters, while decrease the amount of sulfide, which are associated with the oxidation and desulfurization mechanisms.

4.6.2. Molecular weight distribution

From the viewpoint of polymer science, the molecular weight of material is strongly related to its thermodynamics and rheological properties. Fig. 15 presents the GPC curves of CRMB binders with various swelling-degradation degrees. The correlation graphs regarding the molecular weight with retention time are displayed. From the GPC curves, the swelling and degradation processes both significantly affect the molecular weight distribution of CRMB binder. The partial-swelling, full-swelling and partial-degradation CRMB binders exhibit the similar GPC curves, which is related to the less degradation degree. However, the full-degradation sample displays the different molecular weight distribution, especially at the region of high molecular weight. Before conducting the GPC test, the solid insoluble from rubber particles was filtered. Due to the less degradation degree in S0.5, S8 and D7.5, their GPC curves mainly come from the bitumen matrix. Regarding the full-degradation sample, more soluble molecules in rubber particles are released into bitumen phase, which leads to the change of molecular weight distribution.

The influence of swelling degree on the molecular weight distribution of CRMB binder is more apparent when the retention time is less than 28 min and the molecular weight is higher than 5000 Dalton. With the increase of swelling degree, the number of macromolecules increases gradually. The rubber particles would absorb the light-components from the bitumen matrix, which results in the increase of average molecular weight of bitumen phase. Compared to the swelling sample, the GPC curve of full-degradation CRMB shows the distinct peaks before the retention time of 26 min. It implies that the macromolecules with the molecular weight larger than 14,000 Dalton can be detected during the degradation process of CRMB binder. The depolymerization reaction of rubber particles would generate the macromolecules dissolved in bitumen, which is consistent with the FTIR results. Interestingly, the normalized refractive index of oily-components with the molecular weight lower than 14,000 Dalton in full-degradation CRMB binder is smaller than that in swelling samples, which results from the enhanced macromolecules fraction. Meanwhile, the oxidative aging of bitumen would also occur during the long-term degradation mixing process of

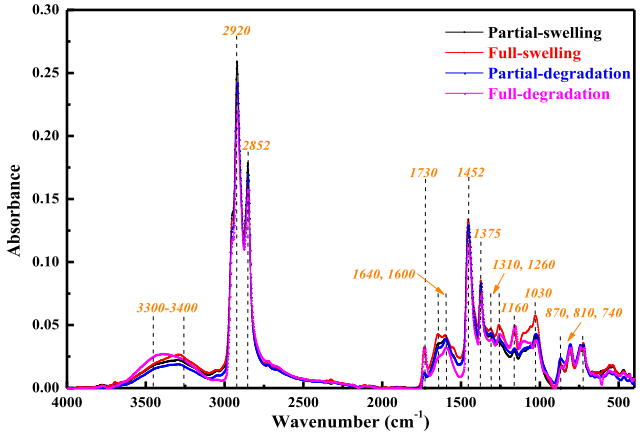

Fig. 14. FTIR results of CRMB binders.

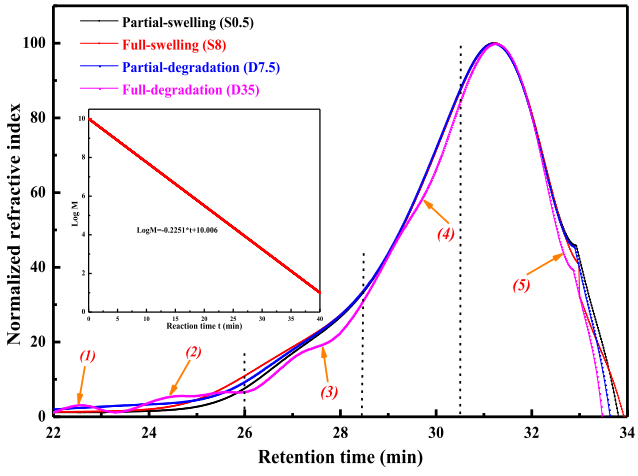

Fig. 15. The molecular weight distribution of CRMB binders.

CRMB binder, which contributes to the reduction of light-component fraction and increase the average molecular weight.

$$M_w = \frac{\sum_{i=1}^{n} w_i \times M_i}{\sum_{i=1}^{n} w_i} \quad (5)$$

$$M_n = \frac{\sum_{i=1}^{n} N_i \times M_i}{\sum_{i=1}^{n} N_i} \quad (6)$$

$$D = \frac{M_w}{M_n} \quad (7)$$

To quantitatively assess the influence of swelling-degradation degree, two average molecular weight of liquid phase (bitumen and dissolved rubber components) are measured. The weight-average molecular weight M_w, number-average molecular weight M_n and dispersion parameter D are calculated by Eqs. (5), (6) and (7), respectively, which are listed in Table 6. The swelling-degradation degree remarkably influences the average molecular weight of liquid phase in CRMB binder, especially for the weight-average molecular weight. The swelling degree increases the average molecular weight of liquid phase in CRMB binder, which decreases during the degradation procedure. Moreover, the dispersion ability of CRMB binder weakens as the swelling degree deepening, and the CRMB binder with high degradation degree would exhibit better dispersion capacity.

5. Conclusions and recommendations

This study explored the continuous swelling and degradation behaviors of CRMB binders with different rubber sizes for the first time and investigated the synergistic effects of swelling-degradation degree and rubber size on the physical, rheological and chemical properties of CRMB binders. The results from this study is beneficial to provide the guidance to optimize the preparation conditions of CRMB binders with different viscosity requirements. The main findings are as follows:

(1) The rubber size shows great influence on the swelling and degradation behaviors of CRMB binder. As the rubber size decreasing, the equilibrium swelling and degradation time are both shortened and the viscosity of CRMB binder is improved dramatically. Moreover, the reduction of rubber size could accelerate the continuous swelling rate, increase the maximum viscosity and shorten the continuous swelling time during the degradation procedure.

(2) The viscosity-based exponential swelling and degradation models are proposed. In the swelling model, the reduction of rubber size increases the absolute values of A and B parameters, but decreases the C value gradually. Meanwhile, in the degradation model, the reduction of rubber size would increase the absolute values of a and b parameters.

(3) The full-swelling CRMB binders exhibit the lower penetration and ductility, which are improved as the rubber size decreasing. The CRMB binder with small rubber size and high degradation degree would exhibit better low-temperature cracking resistance and workability. Additionally, the high swelling degree and large rubber size is beneficial to the high temperature property of CRMB binder.

(4) As the degradation degree deepening, the complex modulus, rutting resistance, elastic property and zero-shear viscosity of CRMB binder are all weakened. Moreover, the frequency dependency of complex modulus and Newtonian flow region of CRMB binder both tend to increase during the degradation procedure. In addition, the reduction of rubber size potentially deteriorates the high temperature properties, but enlarges the Newtonian flow range and improve the workability of CRMB binder.

(5) The swelling degree exhibits no obvious influence on the functional group distribution of CRMB binder. However, the degradation degree promotes the formation of free hydroxide groups, aldehydes, carboxylic acids and esters. Furthermore, the swelling process increases the average molecular weight of whole liquid phase in CRMB binder, which decreases as the degradation degree increasing. However, the macromolecules released from rubber particles are detected in full-degradation sample.

Table 6
Effects of swelling-degradation degree on molecular weight of CRMB binders.

Samples	S0.5	S8	D7.5	D35
M_w (Dalton)	3639	4139	4383	3209
M_n (Dalton)	919	987	936	920
D	3.96	4.19	4.68	3.49

In future works, the influence of bitumen and rubber compositions on the swelling-degradation behaviors of CRMB binder will be studied. Meanwhile, the molecular interaction between the crumb rubber and bitumen during the swelling and degradation procedures could be explored with different multiscale methods. Finally, the synthetic effects of swelling-degradation degree and rubber size of CRMB binder on the mechanical properties of asphalt mixtures should be further investigated.

CRediT authorship contribution statement

Shisong Ren: Formal analysis, Investigation, Methodology, Writing – original draft, Writing – review & editing. **Xueyan Liu:** Supervision, Writing – review & editing. **Peng Lin:** Methodology, Supervision, Writing – review & editing. **Haopeng Wang:** Writing – review & editing. **Weiyu Fan:** Resources, Methodology, Writing – review & editing. **Sandra Erkens:** Supervision.

Declaration of Competing Interest

The authors declare that they have no known competing financial interests or personal relationships that could have appeared to influence the work reported in this paper.

Acknowledgments

The first author would like to thank the funding support from China Scholarship Council (No. 201906450025).

References

[1] V.H. Nanjegowda, K.P. Biligiri, Recyclability of rubber in asphalt roadway systems: a review of applied research and advancement in technology, Resour. Conserv. Recycl. 155 (2020) 104655, https://doi.org/10.1016/j.resconrec.2019.104655.
[2] D.R. Merkel, W. Kuang, D. Malhotra, G. Petrossian, L. Zhong, K.L. Simmons, J. Zhang, L. Cosimbescu, Waste PET chemical processing to terephthalic amides and their effect on asphalt performance, ASC Sustain. Chem. Eng. 8 (14) (2020) 5615–5625, https://doi.org/10.1021/acssuschemeng.0c00036.
[3] S. Ren, X. Liu, H. Wang, W. Fan, S. Erkens, Evaluation of rheological behaviors and anti-aging properties of recycled asphalts using low-viscosity asphalt and polymers, J. Cleaner Prod. 253 (2020) 120048, https://doi.org/10.1016/j.jclepro.2020.120048.
[4] H. Ding, S.A.M. Hesp, Balancing the use of wax-based warm mix additives for improved asphalt compaction with long-term pavement performance, ACS Sustain. Chem. Eng. 9 (21) (2021) 7298–7305, https://doi.org/10.1021/acssuschemeng.1c01242.
[5] A. Ghavibazoo, M. Abdelrahman, Effect of crumb rubber dissolution on low-temperature performance and aging of asphalt-rubber binder, Transp. Res. Rec. J. Transp. Res. Board 2445 (1) (2014) 47–55, https://doi.org/10.3141/2445-06.
[6] A. Milad, A.S.B. Ali, N.I.M. Yusoff, A review of the utilization of recycled waste material as an alternative modifier in asphalt mixture, Civil Eng. J. 6 (2020) 42–60, https://doi.org/10.28991/cej-2020-SP(EMCE)-05.
[7] L.G. Picado-Santos, S.D. Capitão, J.M.C. Neves, Crumb rubber asphalt mixtures: a literature review, Constr. Build. Mater. 247 (2020) 118577, https://doi.org/10.1016/j.conbuildmat.2020.118577.
[8] A.A. Kadhim, H.M.K. Al-Mutairee, An experimental study on behavior of sustainable rubberized concrete mixes, Civil Eng. J. 6 (7) (2020) 1273–1285, https://doi.org/10.28991/cej-2020-03091537.
[9] C. Li, A. Rajib, M. Sarker, R. Liu, E.H. Fini, J. Cai, Balancing the aromatic and ketone content of bio-oils as rejuvenators to enhance their efficacy in restoring properties of aged bitumen, ACS Sustain. Chem. Eng. 9 (20) (2021) 6912–6922, https://doi.org/10.1021/acssuschemeng.0c09131.

[10] X. Ding, T. Ma, W. Zhang, D. Zhang, Experimental study of stable crumb rubber asphalt and asphalt mixture, Constr. Build. Mater. 157 (2017) 975–981, https://doi.org/10.1016/j.conbuildmat.2017.09.164.
[11] R. Balamuralikrishnan, J. Saravanan, Effect of addition of alccofine on the compressive strength of cement mortar cubes, Emerg. Sci. J. 5 (2) (2021) 155–170, https://doi.org/10.28991/esj-2021-01265.
[12] Y. Zhang, Z. Zhang, A.M. Wemyss, C. Wan, Y. Liu, P. Song, S. Wang, Effective thermal-oxidative reclamation of waste tire rubbers for producing high-performance rubber composites, ACS Sustain. Chem. Eng. 8 (24) (2020) 9079–9087, https://doi.org/10.1021/acssuschemeng.0c02292.
[13] M. Liang, X. Xin, W. Fan, H. Sun, Y. Yao, B. Xing, Viscous properties, storage stability and their relationships with microstructure of tire scrap rubber modified asphalt, Constr. Build. Mater. 74 (2015) 124–131, https://doi.org/10.1016/j.conbuildmat.2014.10.015.
[14] S. Wang, D. Cheng, F. Xiao, Recent developments in the application of chemical approaches to rubberized asphalt, Constr. Build. Mater. 131 (2017) 101–113, https://doi.org/10.1016/j.conbuilmat.2016.11.077.
[15] C. Sangiorigi, S. Eskandarsefat, P. Tataranni, A. Simone, V. Vignali, C. Lantieri, G. Dondi, A complete laboratory assessment of crumb rubber porous asphalt, Constr. Build. Mater. 132 (2017) 500–507, https://doi.org/10.1016/j.conbuildmat.2016.12.016.
[16] M.R. Pouranian, M.A. Notani, M.T. Tabesh, B. Nazeri, M. Shishehbor, Rheological and environmental characteristics of crumb rubber asphalt binders containing non-foaming warm mix asphalt additives, Constr. Build. Mater. 238 (2020) 117707, https://doi.org/10.1016/j.conbuildmat.2019.117707.
[17] M. Tausif, S.B.A. Zaidi, N. Ahmad, M.S. Jameel, Influence of natural zeolite and paraffine wax on adhesion strength between bitumen and aggregate, Civil Eng. J. 6 (4) (2020) 733–742, https://doi.org/10.28991/cej-2020-03091505.
[18] J. Ma, M. Hu, D. Sun, T. Lu, G. Sun, S. Ling, L. Xu, Understanding the role of waste cooking oil residue during the preparation of rubber asphalt, Resour. Conserv. Recycl. 167 (2021) 105235, https://doi.org/10.1016/j.resconrec.2020.105235.
[19] P. Xu, J. Gao, J. Pei, Z. Chen, J. Zhang, R. Li, Research on highly dissolved rubber asphalt prepared using a composite waste engine oil addition and microwave desulfurization method, Constr. Build. Mater. 282 (2021) 122641, https://doi.org/10.1016/j.conbuildmat.2021.122641.
[20] C. Qian, W. Fan, Evaluation and characterization of properties of crumb rubber/SBS modified asphalt, Mater. Chem. Phys. 253 (2020) 123319, https://doi.org/10.1016/j.matchemphys.2020.123319.
[21] A. Ameli, R. Babagoli, S. Asadi, N. Norouzi, Investigation of the performance properties of asphalt binders and mixtures modified by crumb rubber and gilsonite, Constr. Build. Mater. 279 (2021) 122424, https://doi.org/10.1016/j.conbuildmat.2021.122424.
[22] Z. Leng, R.K. Padhan, A. Sreeram, Production of a sustainable paving material through chemical recycling of waste PET into crumb rubber modified asphalt, J. Cleaner Prod. 180 (2018) 682–688, https://doi.org/10.1016/j.jclepro.2018.01.171.
[23] M. Liang, X. Xin, W. Fan, S. Ren, J. Shi, H. Luo, Thermo-stability and aging performance of modified asphalt with crumb rubber activated by microwave and TOR, Mater. Des. 127 (2017) 84–96, https://doi.org/10.1016/j.matdes.2017.04.060.
[24] D. Dong, X. Huang, X. Li, L. Zhang, Swelling process of rubber in asphalt and its effect on the structure and properties of rubber and asphalt, Constr. Build. Mater. 29 (2012) 316–322, https://doi.org/10.1016/j.conbuildmat.2011.10.021.
[25] H. Wang, X. Liu, P. Apostolidis, S. Erkens, T. Scarpas, Numerical investigation of rubber swelling in bitumen, Constr. Build. Mater. 214 (2019) 506–515, https://doi.org/10.1016/j.conbuildmat.2019.04.144.
[26] H. Yu, Z. Leng, Z. Zhang, D. Li, J. Zhang, Selection absorption of swelling rubber in hot and warm asphalt binder fractions, Constr. Build. Mater. 238 (2020), 117727, https://doi.org/10.1016/j.conbuildmat.2019.117727.
[27] M.A. Abdelrahman, S.H. Carpenter, Mechanism of interaction of asphalt cement with crumb rubber modifier, Transp. Res. Rec. J. Transp. Res. Board 1661 (1) (1999) 106–113, https://doi.org/10.3141/1661-15.
[28] C. Xia, M. Chen, J. Geng, X. Liao, Z. Chen, G. Zhao, Swelling and degradation characteristics of crumb rubber modified asphalt during processing, Math. Probl. Eng. 2021 (2021) 1–10, https://doi.org/10.1155/2021/6682905.
[29] X. Yang, A. Shen, B. Li, H. Wu, Z. Lyu, H. Wang, Z. Lyu, Effect of microwave-activated crumb rubber on reaction mechanism, rheological properties, thermal stability, and released volatiles of asphalt binder, J. Cleaner Prod. 248 (2020), 119230, https://doi.org/10.1016/j.clepro.2019.119230.
[30] W. Huang, P. Lin, N. Tang, J. Hu, F. Xiao, Effect of crumb rubber degradation on components distribution and rheological properties of terminal blend rubberized asphalt binder, Constr. Build. Mater. 151 (2017) 897–906, https://doi.org/10.1016/j.conbuildmat.2017.03.229.
[31] P. Li, Z. Ding, P. Zou, A. Sun, Analysis of physico-chemical properties for crumb rubber in process of asphalt modification, Constr. Build. Mater. 138 (2017) 418–426, https://doi.org/10.1016/j.conbuildmat.2017.01.107.
[32] A. Ghavibazoo, M. Abdelrahman, Composition analysis of crumb rubber during interaction with asphalt and effect on properties of binder, Int. J. Pavement Eng. 14 (5) (2013) 517–530, https://doi.org/10.1080/10298436.2012.721548.
[33] W.H. Daly, S.S. Balamurugan, I. Negulescu, M. Akentuna, L. Mohammad, S. B. Cooper, S.B. Cooper, G.L. Baumgardner, Characterization of crumb rubber modifiers after dispersion in asphalt binders, Energy Fuels 33 (4) (2019) 2665–2679, https://doi.org/10.1021/acs.energyfuels.8b03559.
[34] P. Li, X. Jiang, Z. Ding, J. Zhao, M. Shen, Analysis of viscosity and composition properties for crumb rubber modified asphalt, Constr. Build. Mater. 169 (2018) 638–647, https://doi.org/10.1016/j.conbuilmat.2018.02.174.
[35] Y. Lei, Z. Wei, H. Wang, Z. You, X. Yang, Y. Chen, Effect of crumb rubber size on the performance of rubberized asphalt with bio-oil pretreatment, Constr. Build. Mater. 285 (2021) 122864, https://doi.org/10.1016/j.conbuildmat.2021.122864.
[36] F. Xiao, S.N. Amirkhanian, J. Shen, B. Putman, Influences of crumb rubber size and type on reclaimed asphalt pavement (RAP) mixtures, Constr. Build. Mater. 23 (2) (2009) 1028–1034, https://doi.org/10.1016/j.conbuildmat.2008.05.002.
[37] J. Huang, Q. Wang, Influence of crumb rubber particle sizes on rutting, low temperature cracking, fracture, and bond strength properties of asphalt binder, Mater. Struct. 54 (2021) 54, https://doi.org/10.1617/s11527-021-01647-4.
[38] ASTM D5-06, Standard Test Method for Penetration of Bituminous Materials.
[39] ASTM D36-06, Standard Test Method for Softening Point of Bitumen (Ring and Ball Apparatus).
[40] ASTM D113-99, Standard Test Method for Ductility of Bituminous Materials.
[41] AASHTO T240, Standard Method of Test for Effect of Heat and Air on a Moving Film of Asphalt (Rolling Thin-Film Oven Test).
[42] AASHTO R28, Standard Method of Test for Accelerated Aging of Asphalt Binder Using a Pressurized Aging Vessel (PAV).
[43] AASHTO T316, Standard Method of Test for Viscosity Determination of Asphalt Binder Using Rotational Viscometer.
[44] AASHTO T315, Standard Method of Test for Determining the Rheological Properties of Asphalt Binder Using a Dynamic Shear Rheometer (DSR).
[45] AASHTO MP19, Standard specification for Performance-Graded Asphalt Binder Using Multiple Stress Creep Recovery (MSCR) Test.
[46] S. Ren, X. Liu, W. Fan, C. Qian, G. Nan, S. Erkens, Investigating the effects of waste oil and styrene-butadiene rubber on restoring and improving the viscoelastic, compatibility, and aging properties of aged asphalt, Constr. Build. Mater. 269 (2021) 121338, https://doi.org/10.1016/j.conbuildmat.2020.121338.
[47] C. Yan, W. Huang, J. Ma, J. Xu, Q. Lv, P. Lin, Characterizing the SBS polymer degradation within high content polymer modified asphalt using ATR-FTIR, Constr. Build. Mater. 233 (2020) 117708, https://doi.org/10.1016/j.conbuildmat.2019.117708.
[48] P. Lin, W. Huang, N. Tang, F. Xiao, Y. Li, Understanding the low temperature properties of terminal blend hybrid asphalt through chemical and thermal analysis methods, Constr. Build. Mater. 169 (2018) 543–552, https://doi.org/10.1016/j.conbuildmat.2018.02.060.